



HAL
open science

A 3D-fem model solving thermomechanics and macrosegregation in binary alloys solidification

Michel Bellet, Victor D. Fachinotti, Sylvain Gouttebroze, Weitao Liu, Hervé Combeau

► **To cite this version:**

Michel Bellet, Victor D. Fachinotti, Sylvain Gouttebroze, Weitao Liu, Hervé Combeau. A 3D-fem model solving thermomechanics and macrosegregation in binary alloys solidification. Symposium on Solidification Processes and Microstructures in Honor of Wilfried Kurz held at the TMS Annual Meeting, Mar 2004, Charlotte, United States. pp.Pages 41-46 - ISBN: 0-87339-572-7. hal-00531333

HAL Id: hal-00531333

<https://minesparis-psl.hal.science/hal-00531333>

Submitted on 11 Mar 2011

HAL is a multi-disciplinary open access archive for the deposit and dissemination of scientific research documents, whether they are published or not. The documents may come from teaching and research institutions in France or abroad, or from public or private research centers.

L'archive ouverte pluridisciplinaire **HAL**, est destinée au dépôt et à la diffusion de documents scientifiques de niveau recherche, publiés ou non, émanant des établissements d'enseignement et de recherche français ou étrangers, des laboratoires publics ou privés.

A 3D-FEM MODEL SOLVING THERMOMECHANICS AND MACROSEGREGATION IN BINARY ALLOYS SOLIDIFICATION

Michel Bellet¹, Victor D. Fachinotti¹, Sylvain Gouttebroze¹, Weitao Liu², Hervé Combeau²

¹Ecole des Mines de Paris, CEMEF, UMR CNRS 7635, Sophia Antipolis, France

²Ecole des Mines de Nancy, LSG2M, Parc de Saurupt, Nancy, France

Keywords: macrosegregation, solidification, finite elements, 3D

Abstract

This paper introduces a three-dimensional numerical model for the coupled solution of momentum, energy and solute conservation equations, for binary alloys solidification. The spatial discretisation is carried out using linear tetrahedral finite elements, particularly those of P1+/P1 type for the velocity-pressure resolution of momentum equation. The liquid flow in the mushy zone is assumed to be governed by the Darcy's law. Thermal and buoyancy forces are taken into account by means of the Boussinesq's model. Microsegregation obeys the lever rule. The resulting solute transport equation is solved by the SUPG method. Coupling strategy between momentum, energy and solute equations is discussed and two applications are studied.

Introduction

Conservation equations over the two-phase mushy domain involved in alloy solidification may be obtained either by the classical mixture theory [1,2] or by spatial averaging techniques [3,4]. While the former gives rise to simpler single-phase-like equations, the latter clarifies the relationship between macro and microscopic scale phenomena. The main objective of the present work is the prediction of the macrosegregation pattern in solidifying binary alloys. We present here the strategy adopted in THERCAST[®], a 3D finite-element code developed by CEMEF, in collaboration with LSG2M. The results for a test case will be compared with those of SOLID, a finite volume two-dimensional code developed by Combeau *et al* [5].

1 Governing equations and resolution

The analysis of fluid flow, temperature and solute distribution in a solidifying material amounts to the coupled solution of the equations stating the conservation of mass, momentum, energy and solute in the domain occupied by the material.

Simplifying hypotheses

The present model of binary-alloy solidification is based upon the following hypotheses. We refer to [6] for a discussion on the range of validity of these assumptions.

- The liquid flow is laminar, Newtonian, with a constant-viscosity μ . The solid phase is fixed and non deformable.
- The mushy region is modeled as an isotropic porous medium saturated with liquid (*i.e.*: $g_s + g_l = 1$, g_s denoting the volumic solid fraction and g_l the liquid one). Its permeability K is defined by the Carman-Kozeny formula, in which λ_2 is the secondary dendrite arm spacing: $K = \lambda_2^2 g_l^3 (1 - g_l)^{-2} / 180$.

- The solid and liquid phase densities are equal ($\rho = \rho_s = \rho_l$) and constant ($\rho = \rho_0$), except in the buoyancy term of the momentum equation where density depends on the temperature T and the solute concentration in liquid w_l according to the Boussinesq approximation $\rho = \rho_0(1 - \beta_T(T - T_0) - \beta_w(w_l - w_{l0}))$, in which β_T and β_w are the thermal and solutal expansion coefficients, respectively.
- The microsegregation is governed by the lever rule. Given k the partition coefficient at solid-liquid interface, the average solute concentration w is related to w_l by:

$$w = g_l w_l + g_s k w_l = (g_l + (1 - g_l)k) w_l \quad (1)$$

- The phase diagram is linearized, the liquidus slope m being constant and T_m being the melting temperature of the pure substance, we have:

$$T = T_m + m w_l \quad (2)$$

Mass conservation

Denoting V the average velocity (here equal to the average liquid velocity, since the solid is fixed), the mass conservation equation is reduced to:

$$\nabla \cdot V = 0 \quad (3)$$

Momentum conservation

The classical mixture theory [1, 2] yields (4), while the averaging technique [3, 4] leads to (5):

$$\rho_0 \frac{dV}{dt} = \nabla \cdot (\mu \nabla V) - \nabla p + \rho g - \frac{\mu}{K} V \quad (4)$$

$$\rho_0 \frac{\partial V}{\partial t} + \frac{\rho_0}{g_l} \nabla \cdot (V \times V) = \nabla \cdot (\mu \nabla V) - g_l \nabla p + g_l \rho g - \frac{\mu}{K} g_l V \quad (5)$$

where p is pressure field and g the gravity vector. While the finite volume code SOLID [5], with which our results are compared, is based on (5), THERCAST, originally based on (4), also considers (5). The time-discretized form of (4) and (5) is obtained using the Euler-backward scheme. Spatial discretisation is carried out using mixed P1+/P1 tetrahedral finite elements [7]. Inside each element, the velocity is interpolated by a linear function enriched by a piecewise linear correction (bubble function), while the pressure shape function is linear. An Arbitrary Lagrangian-Eulerian (ALE) strategy [8] is applied in order to account for material advection.

Solute conservation

Redistribution of solute is governed by the equation

$$\frac{\partial w}{\partial t} + V \cdot \nabla w_l - \nabla \cdot (\varepsilon \nabla w_l) = 0 \quad (6)$$

where ε is a diffusion coefficient, usually negligible (and kept arbitrarily small). Following Voller *et al* [6], the time-integrated version of (6) is written as:

$$\frac{w^t - w^{t-\Delta t}}{\Delta t} + \nabla w \cdot V + \nabla \cdot (\varepsilon \nabla w) = \nabla \cdot (w^* - w_l^*) V - \nabla \cdot [\varepsilon \nabla (w^* - w_l^*)] \quad (7)$$

It will be seen further that the super-index * refers either to the value at the previous time instant $t - \Delta t$, in case of weak coupling, or to the latest iterative estimate in case of strong coupling. The weak form of (7) is solved by the Streamline Upwind/Petrov-Galerkin method.

Energy conservation

The heat equation can be written as follows, given the above assumptions:

$$\rho \left(\frac{\partial H}{\partial t} + \nabla H_l \cdot \mathbf{V} \right) - \nabla \cdot (\lambda \nabla T) = 0 \quad (8)$$

where λ is the thermal conductivity and H is the average enthalpy:

$$H = c_p T + g_l L \quad (9)$$

c_p being the specific heat (assumed constant) and L the latent heat. This simply leads to $\nabla H_l = c_p \nabla T$ in (8). Linear tetrahedral elements and a Euler-backward scheme are used to discretise (8) in space and time, respectively. In each element, a constant value of $\partial H / \partial T$ is used, in order to solve a weak form of (8) for the nodal enthalpies, also using SUPG.

Resolution strategy

In the context of a Eulerian (fixed mesh) resolution, the resolution algorithm over a time increment is described in box 1. It can be seen that some resolution steps are iteratively chained in case of full coupling. The superscript * indicates the current estimate during iterations. In case of weak coupling the step 1 is solved with w assumed constant and equal to the local value given by (7) just before the point begins to solidify.

$\mathbf{x}^t, T^t, g_l^t, w^t, w_l^t$: variables known at the beginning of a new time increment	
1) Resolution of energy conservation (weak form of (8))	$\rightarrow H^*$
2) Resolution of solute average conservation (weak form of (7))	$\rightarrow w^*$
3) Local resolution, at each node, of microsegregation ((1), (2) and (9))	$\rightarrow g_l^*, T^*, w_l^*$
4) Resolution of momentum conservation (weak form of (4) or (5))	$\rightarrow \mathbf{V}^*, p^*$
5) If full coupling, iterate steps 1) to 4) until convergence. At the end, assign: $var^{t+\Delta t} \leftarrow var^*$	
6) Transport for particle derivatives, by nodal upwind (see [8])	
7) Updating of variables: $t \leftarrow t + \Delta t, T^t \leftarrow T^{t+\Delta t}, g_l^t \leftarrow g_l^{t+\Delta t}, w^t \leftarrow w^{t+\Delta t}, w_l^t \leftarrow w_l^{t+\Delta t}$	

Box 1: Summary of the main procedures carried out during a time increment.

2 Applications

Binary alloy Fe-0.2wt%C in a square cavity

A cavity of $10 \times 10 \text{ cm}^2$ area, full of 0.2wt%C steel, initially liquid at 1523°C , is cooled down by convection to the environment through the vertical walls. Invoking symmetry, half of the cavity is modeled. Mechanical and thermal boundary conditions, as well as material data are given in fig. 1. For the 3D analysis with THERCAST, a 10 mm-thick slice delimited by symmetry planes is considered. The mesh used for the analysis (3112 nodes), is shown in fig. 1.

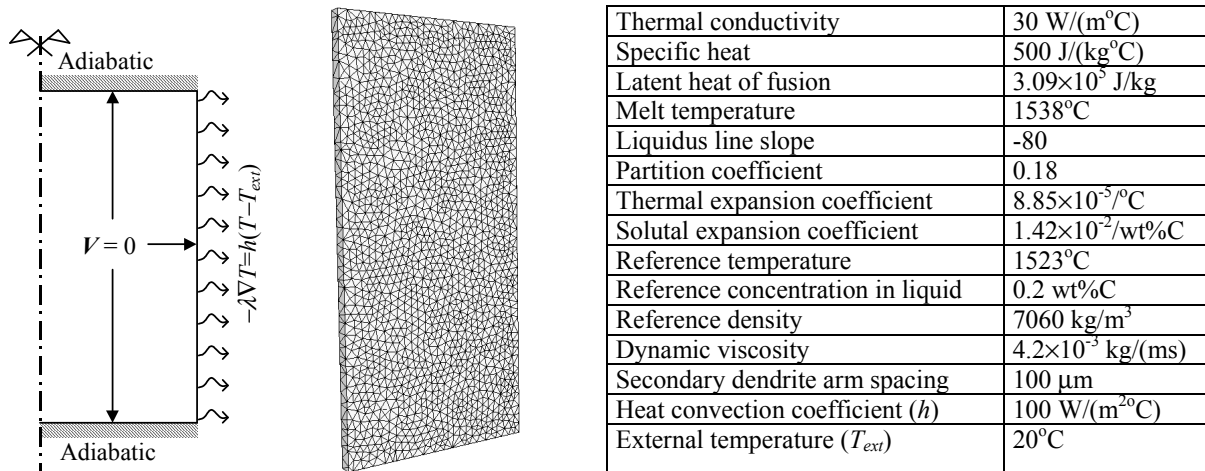


Figure 1. Left: test problem and 3D finite element mesh. Right: thermophysical data.

For the 2D analysis using SOLID, a structured uniform grid was used. A constant time step of 0.1 s was adopted for both 2D and 3D analyses. First, it should be noted that we found no difference in using either the classical mixture theory or the averaging technique (eq. (4) or (5)). This amounts to think of the flow inside the mushy region as completely governed by the Darcy law. However, more work would be necessary to extend this conclusion to other configurations. Macrosegregation patterns in the cavity once it is totally solidified ($t=1000$ s) are plotted in fig. 2. Both SOLID and THERCAST solutions are in good agreement. The extreme values of positive and negative segregation (*i.e.*, $w>0.2\%$ and $w<0.2\%$, respectively) predicted by THERCAST are higher than those of SOLID. Let us note that similar differences between SOLID finite-volume approach and a 2D finite-element code have been previously reported in [4].

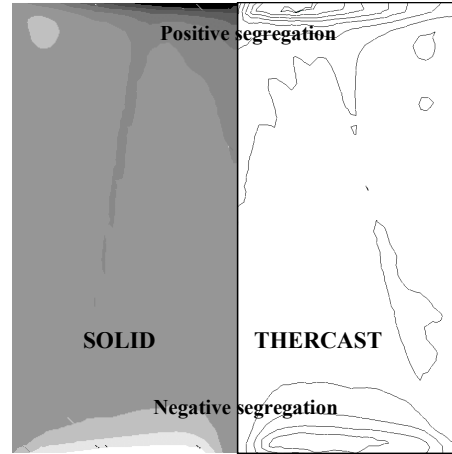


Figure 2. Macrosegregation at 1000 s. SOLID range: 0.195%-0.208%, THERCAST range: 0.193%-0.209%.

Hebditch and Hunt test

The second case consists of the solidification of Pb-48wt%Sn and Sn-5wt%Pb ingots studied by Hebditch and Hunt [9]. In this test, the alloy is solidified in a parallelepipedic cavity (6 cm high, 10 cm long and 1.3 cm thick, see fig. 3), which is isolated on all surfaces except the thinnest lateral one. This test has already served as a benchmark to evaluate the results of 2D and 3D solidification codes [4, 10]. Here it is studied with the two-dimensional version of THERCAST, also named R2SOL, in order to evaluate the coupling strategy (such a study is more easily carried out in 2D, because of shorter computation times). In this case, we assume that the fluid flow in the largest midplane section is not influenced by the two parallel walls of the cavity. The physical data used in the calculation can be found in the literature [4].

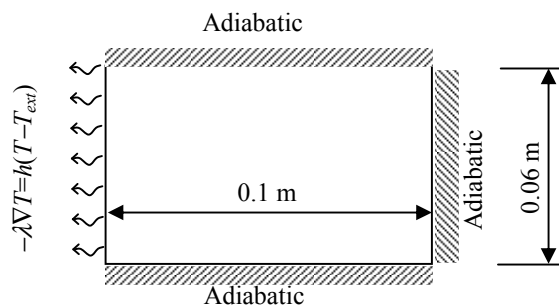


Figure 3. Hebditch and Hunt test problem.

Sn-5wt%Pb alloy

The computation is performed with a non-structured mesh (5440 nodes, see fig. 4) and a constant time step of 0.05 s, which is the same as in SOLID. The maximum number of iterations within each time step is limited to 10 for the fully coupled approach. The difference between the weak and full coupling is illustrated. It can be seen that the segregated channels shown by the finite volume code SOLID are much less obvious on the finite element results. Their tendency to form is predicted only by the fully coupled approach. Moreover, as shown in fig. 4c, the finite element computation with a structured mesh shows no channels. These results are partially consistent with those in [4], and clearly requires deeper investigation.

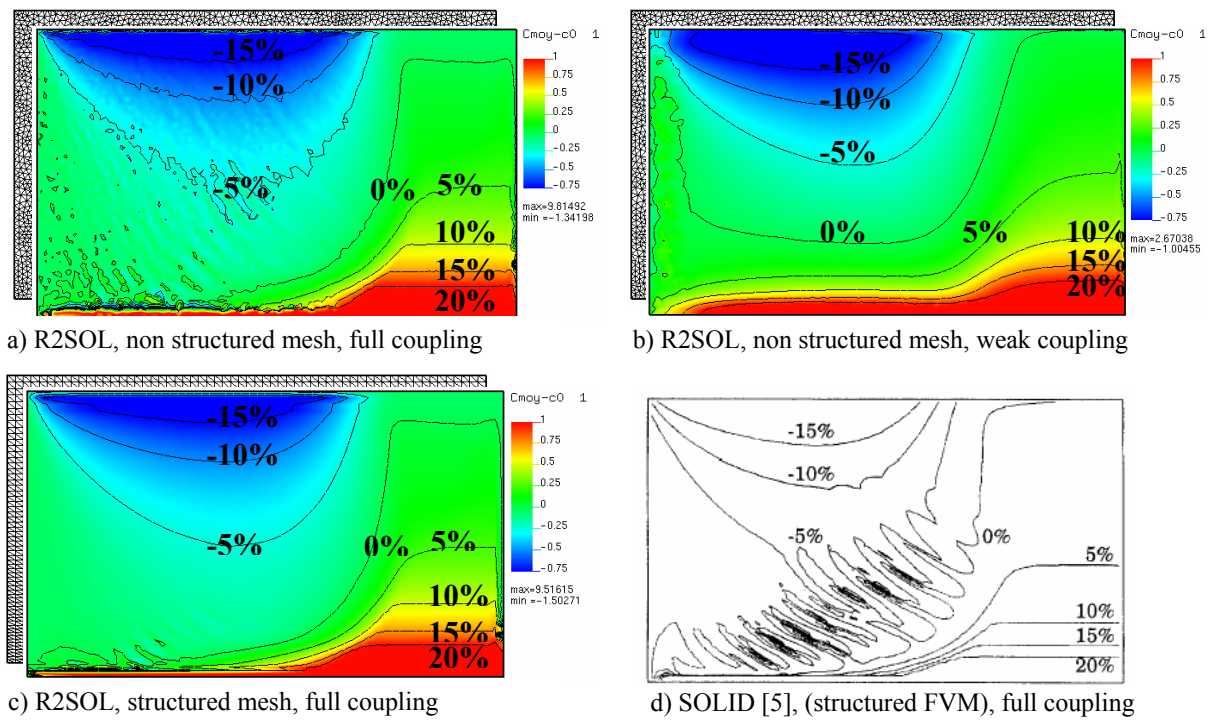


Figure 4. Relative variation of Pb average concentration at 400 s.

Pb-48wt%Sn alloy

The calculation is run with a non structured finite element mesh (2023 nodes), a time step of 0.1 s and the fully coupled approach. The liquid fraction at 50 s and the segregation at 400 s are plotted in fig. 5. The results are close to those of SOLID. Some of the differences between finite volumes and finite elements are due to the treatment of the non-slip boundary condition, as explained in [4]. Other differences can be seen at the top of the cavity: some wiggles initiate near the solidification front in the finite element solution. They are not shown by a computation with a finite element structured mesh.

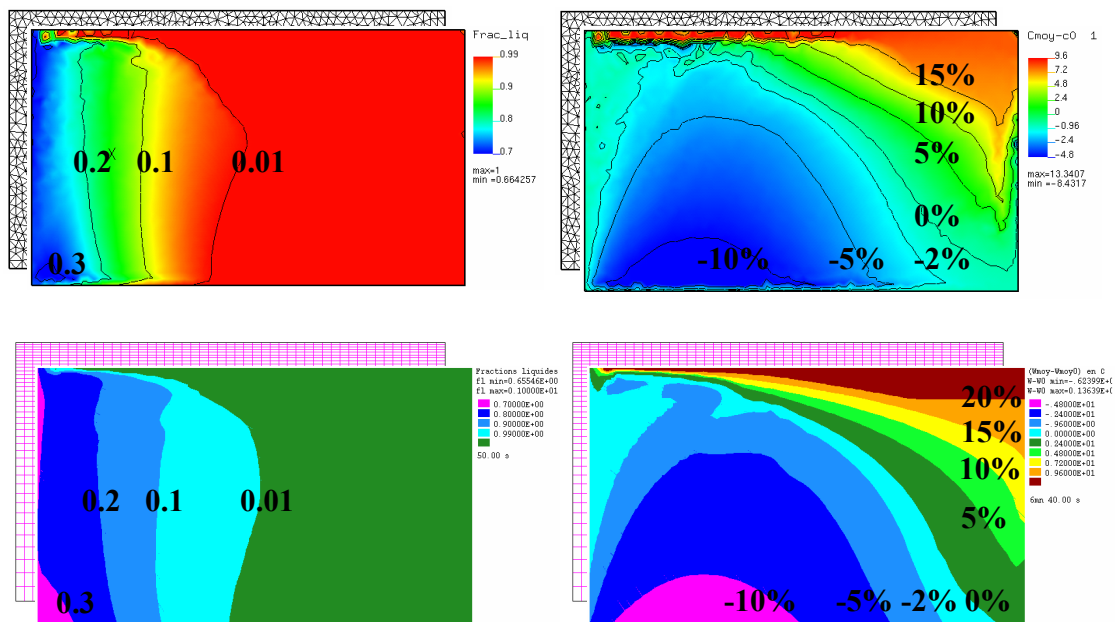


Figure 5. On the left, maps of the solid fraction at 50 s obtained by R2SOL and SOLID (both with full coupling). On the right, corresponding relative variation of Sn concentration at 400 s.

The concentration profiles in different sections of the specimen at the end of the solidification are shown in fig. 6. Measurements and numerical predictions are in good agreement, except in the top section, where the variations are important (as well as the measurement inaccuracy, particularly because of specimen deformation [9]).

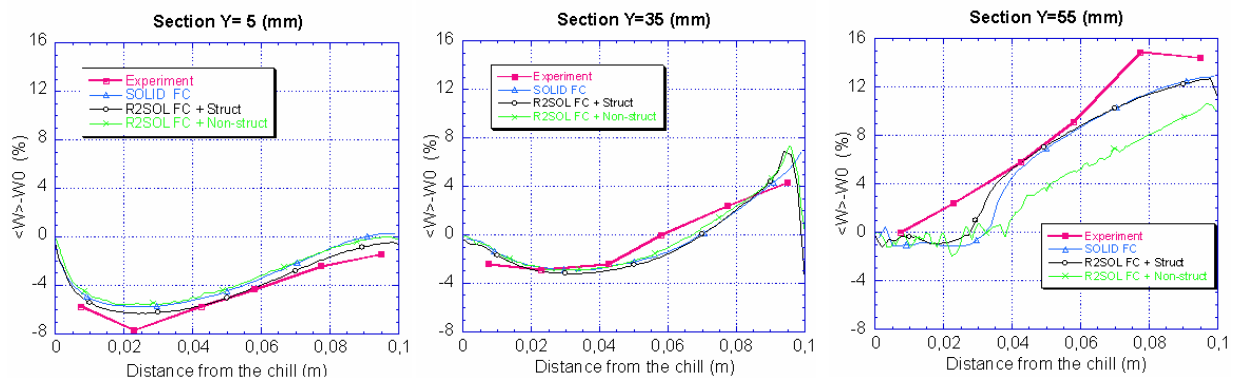


Figure 6. Profiles of Sn concentration at the end of solidification in three horizontal sections. Measurements and results obtained by the full coupling approaches of R2SOL and SOLID.

Conclusion

A first implementation of macrosegregation modelling has been implemented in THERCAST software. Future work will be dedicated to deeper investigations regarding mesh influence, to the extension to multiconstituent alloys and to the application to industrial castings.

Acknowledgement

This work has been supported by the French Ministry of Industry, the French Technical Center of Casting Industries (CTIF) and the companies Arcelor-Irsid, Ascometal, Fonderie Atlantique Industrie, Aubert et Duval Alliages, Erasteel, Industeel and PSA. Victor D. Fachinotti is also granted by the Argentine Council for Scientific and Technical Research (CONICET).

References

1. C. Prakash and V. Voller, On the Numerical Solution of Continuum Mixture Equations Describing Binary Solid-Liquid Phase Change, *Num. Heat Transfer B* 15 (1989) 171-189.
2. W.D. Bennon and F.P. Incropera, A Continuum Model for Momentum, Heat and Species Transport in Binary Solid-Liquid Phase Change Systems – I. Model Formulation, *Int. J. Heat Mass Transfer* 30 (1987) 2161-2170.
3. J. Ni and C. Beckermann, A Volume-Averaged Two-Phase Model for Transport Phenomena during Solidification, *Metall. Trans.* 22B (1991) 349-361.
4. N. Ahmad, H. Combeau, J.-L. Desbiolles, T. Jalanti, G. Lesoult, M. Rappaz and C. Stomp, Numerical Simulation of Macrosegregation: a Comparison between Finite Volume Method and Finite Element Method Predictions and a Confrontation with Experiments, *Metall. and Mat. Trans.* 29A (1997) 617-630.
5. H. Combeau, F. Roch, J. C. Chevrier, I. Poittraut and G. Lesoult, Numerical Study of Heat and Mass transfer during Solidification of Steel Ingots, In: *Advanced Computational Methods in Heat Transfer*, ed. L. C. Wrobel, Springer-Verlag, New York (1990) 79-90.
6. V.R. Voller, A.D. Brent, C. Prakash, The Modelling of Heat, Mass and Solute Transport in Solidification Systems, *Int. J. Heat Mass Transfer* 32 (1989) 1719-1731.
7. D.N. Arnold, F. Brezzi, M. Fortin, A Stable Finite Element Method for the Stokes Equations, *Calcolo* 21 (1984) 337-344.
8. M. Bellet, V.D. Fachinotti, ALE method for solidification modeling, to be published in *Comp. Meth. Appl. Mech. Engng.*
9. D.J. Hebditch, J.D. Hunt, Observations of ingot macrosegregation on model systems. *Metall. Trans.* 5 (1974) 1557-1564.
10. J.L. Desbiolles, P. Thevoz, M. Rappaz, *Micro-/Macrosegregation modeling in casting: a fully coupled 3D model*. Proc. of Modeling of Casting, Welding and Advanced Solidification Processes X, TMS (2003) 245-252.